Generation of nanoflowers and nanoneedles on Co-based layered perovskite of IT-SOFC cathode affecting electrical conductivities

Ji Min Im [a], Kyeong Eun Song [a, b], Harald Schlegl [c], Hyunil Kang [d], Wonseok Choi [d], Seunug-Wook Baek [e], Jun-Young Park [f], Hyun-Suk Kim [g], Jung Hyun Kim [a,*]

[a] Department of Advanced Materials Science and Engineering, Hanbat National University, 125, Dongseo-Daero, Yuseong-Gu, Daejeon, 34158, Republic of Korea

[b] Fuel Cell Innovations Co., Ltd. 41-7, Techno 11-ro, Yuseong-gu, Daejeon, Republic of Korea

[c] Physics Department, Lancaster University, Bailrigg, Lancaster LA1 4YB, United Kingdom

[d] Department of Electrical Engineering, Hanbat National University, 125, Dongseo-Daero, Yuseong-Gu, Daejeon, 34158, Republic of Korea

[e] Interdisciplinary Materials Measurement Institute, Korea Research Institute of Standards and Science (KRISS), 267, Gajeong-Ro, Yuseong-Gu, Daejeon, 34113, Republic of Korea

[f] HMC, Department of Nanotechnology and Advanced Materials Engineering, Sejong University, Seoul 05006, Republic of Korea

[g] Department of Materials Science and Engineering, Chungnam National University, Daejeon, 34134, Republic of Korea

Corresponding author:*

Jung Hyun Kim: jhkim2011@hanbat.ac.kr, jhkim1870@gmail.com,

Tel: +82-42-821-1239, Fax: +82-42-821-1592,

Department of Advanced Materials Science and Engineering, Hanbat National University, 125,

Dongseo-Daero, Yuseong-Gu, Daejeon, 34158, Republic of Korea

Abstract

In this study, the unusual microstructure and electrical properties of $SmBa_{0.5}Sr_{0.5}Co_2O_{5+d}$ (SBSCO) layered perovskite cathodes with dense and porous microstructures were analyzed by changing the applied current.

Unique nanostructure shapes were observed when a high current was applied to a cathode with both dense and porous microstructures of the same chemical composition for electrical conductivity measurement. Nanoflower and nanoneedles, which are types of nanoseeds, were discovered. The nanoneedles were found on the entire surface of the SBSCO cathode, whereas nanoflowers were only present on part of the cathode surface.

Results from an Energy Dispersive Spectrometer (EDS) analysis revealed that the nanoneedles generated on the SBSCO matrix had a chemical composition of $SmBaCo_2O_{5+d}$ (SBCO).

The electrical conductivity of the porous cathode with SBCO nanoneedles (nanoneedle cathode) was 238 S/cm at 700 ^oC under decreasing temperature in an air atmosphere (Air Down) during the experiment. In comparison, the electrical conductivity of the porous cathode without nanoneedles (normal cathode) was 136 S/cm at the same experiment condition (700 ^oC, Air Down). This indicates that the electrical conductivity of the nanoneedle cathode was significantly higher than that of the normal cathode.

Keywords: Solid oxide fuel cell (SOFC), Layered perovskite, Cathode, Nanoseed, Nanoneedle, Electrical conductivity

1.Introduction

A Solid Oxide Fuel Cell (SOFC) is a device that directly converts chemical energies of H_2 and O_2 into electrical energy. It is an environmentally friendly power generation device that reduces CO_2 emissions by using hydrogen as an energy source instead of fossil fuels [1, 2]. Compared to other fuel cells, SOFCs have the advantages of high electrical efficiency and high power density due to their ability to operate at high temperatures ranging from 600 ºC to 1000 ºC [3-5]. However, the advantage of the high operating temperature can also be seen as a disadvantage. For example, due to its high-temperature operating characteristics, there are problems such as chemical reactions and phase instability between the materials constituting the SOFC, as well as reduced stability and performance degradation of cells and stacks due to thermal degradation [6, 7].

Therefore, as a key area of research, Intermediate Temperature-operating SOFCs (IT-SOFCs) with relatively lower operating temperature ranges have been studied [8-11]. By reducing the operating temperature to 500 ºC ~ 700 ºC, various material and operating issues at high temperatures can be addressed [12, 13]. This brings the advantages of reducing system operating costs and increasing the life of the stack. However, the main disadvantage of an IT-SOFC is that the cathode resistance contributes more than 50% of the total resistance of all the components [5, 14, 15]. Improving the cathode performance is therefore crucial to enhance the overall performance of the IT-SOFC [16].

Many research methods have been proposed to improve the cathode performance of IT-SOFCs. In particular, many types of research are currently underway to increase the diffusion of oxygen ions and enhance the surface properties by changing the structure of the cathode from an ABO_3-type complex perovskite structure to an $AA'B_2O_{5+d}$ type layered perovskite structure. In particular, the layered perovskite structure, which has the order of $[CoO_2]$-[BaO]-

[CoO_2]-[LnO_6] and is aligned along the c-axis, can improve oxygen ion diffusion through the distribution of oxygen vacancies [17-20].

In addition, studies on the electrochemical properties in relation to the materials and amounts substituted for each site of layered perovskite are also actively underway. For example, regarding the effect of the A-site substitution amount of $LnBa_{0.5}Sr_{0.5}Co_2O_{5+d}$ (A: Lanthanide, $A^{/}$: Ba, Sr), $Sm_{0.2}Nd_{0.8}Ba_{0.5}Sr_{0.5}Co_2O_{5+d}$ has an electrical conductivity of 516 S/cm and ASR of 0.043 Ωcm^2 at 700 ºC. Therefore, a strategic approach of substitution and varying the substitution amount of the substance for the A-site can effectively improve the performance of the IT-SOFC cathode [21].

In addition to these studies, various studies have been conducted to improve the performance of the cathode, such as exposing particles that play a role in the oxygen reduction reaction (ORR) of the cathode to the surface by changing the microstructure of the cathode [22].

Our research group reported that $SmBa_{0.5}Sr_{0.5}Co_2O_{5+d}$ (SBSCO) with a layered perovskite structure, where the A-site is substituted with Sm, the $A^{/}$-site with Ba and Sr, and the B-site with transition metal Co, had an electrical conductivity of 427.8 S/cm and an ASR of 0.09 Ωcm^2 at 700 ºC. The ASR of the composite SBSCO with 50 wt% of $Ce_{0.9}Gd_{0.1}O_{2-d}$ (CGO91) also had an excellent electrochemical property of 0.013 Ωcm^2 at 700 ºC [23].

In addition, a SBSCO cathode with these characteristics was fabricated with two microstructures (dense and porous cathode) and the relationship between the electrochemical properties and microstructure was analyzed. It has been reported that there is a difference in the movement of charge carriers between a porous and a dense cathode due to a difference in the microstructure, which results in differences in electrical conductivity [24].

In this study, the relationship between microstructure and electrical conductivity in a layered perovskite SBSCO cathode was investigated by varying the conditions of oxygen partial

pressure and applied current, resulting in changes in the microstructure. Particles with unique shapes that formed during the microstructural changes were closely studied, and an electrical conductivity analysis was conducted to determine their impact on the cathode performance.

2.Experimental

2.1. Phase Synthesis

Sm_2O_3 (Alfa Aesar, 99.9%), $BaCO_3$ (Samchun, 99.0%), $SrCO_3$ (Aldrich, 99.9%), and Co_3O_4 (Alfa Aesar, 99.7%) were utilized as the primary raw materials to synthesize a $SmBa_{0.5}Sr_{0.5}Co_2O_{5+d}$ (SBSCO) layered perovskite cathode.

To synthesize SBSCO single phase through the traditional solid-state reaction method (SSR), each raw material powder was weighed accurately to the third decimal place and mixed uniformly in an agate mortar. In this process, ethanol was added to prevent the loss of fine powder and scattering.

The mixed material was dried at 78 ºC for 24 hours to evaporate ethanol fully, and underwent the first calcination. The first calcination was performed with a temperature increase rate of 5 °C per minute, reaching 1000 °C and held for six hours. In this process, $BaCO_3$ was reduced to BaO and $SrCO_3$ to SrO, forming a single phase simultaneously. The secondary calcination was performed at 1100 °C for eight hours, synthesizing all unreacted remaining raw material powders into a single phase. The powder was then pulverized to produce SBSCO cathode powder with a layered perovskite structure.

2.2. Sample preparation

2.2.1. Dense and porous samples for microstructure analysis

A dense cathode sample was made by putting 2.5 g of synthesized cathode powder into a rectangular metal mold (25 mm x 6 mm x 4 mm) and pressing with $2x10^3$ kg/m^2. It was then sintered at 1100 °C for three hours in an air atmosphere.

The porous cathode sample was produced using an electrolyte substrate because of two reasons. Firstly the electrical conductivity of the porous cathodes used in this research with a thickness of 20-30 micrometers cannot be measured without the use of an electrolyte support and secondly the porous cathode in the form of a thin film requires mechanical support from the electrolyte substrates. Therefore, the following process is required [24, 25]. First, 9 g of $Ce_{0.9}Gd_{0.1}O_{2-d}$ (CGO91) powder was compressed into a rectangular metal mold (30 x 23 x 2 mm) with 1.5 x 10^3 kg/m^2 pressure to form the electrolyte substrate. The substrate was then heat-treated for six hours at 1450 °C to produce a dense sintered body. The cathode ink was made by mixing 5 g of cathode powder, 0.1 g of KD-1 dispersant, and 100 ml of acetone solvent in a Nalgene bottle. The cathode powder and dispersant were mixed through ball milling at 160 rpm for 24 hours. The zirconia beads were removed from the slurry and the remaining part was stirred at room temperature to form a cathode ink paste. The specific process can be found in a previously published study by our research group [23-28]. The cathode ink was thinly screen-printed on the sintered CGO91 electrolyte substrate using a mesh (23 x 6 mm). Platinum paste was used to print voltage and current lines on the cathode, following the DC 4 probe method. The sample was then heat-treated at 1000 ºC for three hours.

2.2.2. Phase and microstructure analysis

An X-ray diffraction (XRD) analysis was performed to determine the phase of the synthesized powder. The equipment used was a Model D/Max 2500 from Rigaku (45 kV, 200 mA) with Cu Kα radiation. The data obtained confirmed the synthesis of layered perovskite

and the crystallographic information was analyzed using the MDI JADE 6 program [29].

The microstructure of the prepared cathode was analyzed using a scanning electron microscope (SEM, Model: JEOL JSM-IT500). A gold coating was applied to the cathode using the sputtering method to address the surface charging effect and ensure stable SEM measurements. The gold layer was deposited for 40 seconds with an ion current value set at 10 mA. After microstructure observation, Energy Dispersive Spectrometer (EDS, Model: Oxford Ultim Max) measurement was performed to confirm the composition. In this process, transmission electron microscopy (TEM, Model: HITACHI HF5000) images were used.

2.3. Electrical conductivity measurement

In this study, the impact of different current values on the microstructure characteristics of the cathode was analyzed.

When a high current value is applied to the porous cathode, an overvoltage may occur, potentially leading to destruction of the cathode. Thus, a lower current value was applied to the porous cathode compared to the dense cathode because the porous cathode has high porosity, resulting in lower conductivity than the dense cathode.

In addition, the current value at which the porous cathode was destroyed differed in the air atmosphere and nitrogen atmosphere. For example, when assuming that currents corresponding to a high current are applied in a nitrogen atmosphere, an overvoltage may occur in a P-type cathode with low conductivity due to a low oxygen partial pressure, and the porous cathode may be destroyed [24]. Thus, in this condition, the applied current value differed according to the atmosphere condition. Therefore, the electrical conductivity measurement conditions for the porous cathode were referenced from a previous study reported by our research group [24]. That is, in the case of the electrical conductivity measurement experiment conducted by our

research group, currents of 0.05, 0.075, 0.1, and 0.3 A were applied in an air atmosphere and currents of 0.01, 0.02, 0.03, 0.04, and 0.05 A were applied in a nitrogen atmosphere, respectively. For standardization, the total current values for each atmosphere were divided by minutes and set as the high current value.

A Keithley 2400 source meter was used to measure the electrical conductivity of the porous cathode. The sample was connected using a Pt wire and a Pt clamp, and the DC 4 probe method was used. The temperature range was from 50 ^{o}C to 900 ^{o}C with an increment of 50 ^{o}C. Both a heating process (measuring while rising from 50 °C to 900 °C) and a cooling process (opposite of the heating cycle) were performed. During the conductivity measurements, the atmosphere was controlled by supplying air and nitrogen gases, respectively.

To observe the electrical conductivity caused by changes in the microstructure according to applied current values, electrical conductivity measurements were performed by halving the applied current value. For example, the experiment was conducted by setting the applied current values to 0.025, 0.0375, 0.05, and 0.15 A (air atmosphere) and 0.005, 0.01, 0.015, 0.02, and 0.025 A (nitrogen atmosphere), which are half of the previously applied values.

3. Results and discussion

The X-ray diffraction (XRD) results for the SBSCO powder prepared by the solid phase synthesis (SSR) method showed the same results as the SBSCO layered perovskite structure reported by our group [20, 23-26]. Therefore, the microstructure analysis was carried out as the SBSCO was considered to be well compounded.

3.1. Microstructural characteristics according to various experimental conditions

3.1.1. The effect of oxygen partial pressure in dense and porous cathodes

By using two types of cathodes, dense and porous, the microstructural characteristics of each

cathode were evaluated through a SEM analysis. In these experiments, 0.1 A/min was applied when measuring the electrical conductivity of the dense cathode in air and nitrogen atmospheres. On the other hand, in the porous cathode, 0.03 A/min was applied in an air atmosphere and 0.005 A/min was set in a nitrogen atmosphere.

Figure 1 summarizes the microstructural differences between the dense and porous cathode types where the current was applied in air and nitrogen atmospheres. Figure 1 (a) shows the microstructural features of dense SBSCO exposed to air without currents. Particles do not exist on the grain and grain boundary surface of the cathode, and as seen in Figures 1 (b) and (c), when the current was applied to the dense cathode, the surface of the cathode does not show a significant difference from the microstructure of the existing dense SBSCO cathode when compared with Figure 1 (a).

In contrast, Figures 1 (e) and (f) show that when current was applied to the porous cathode, fine particles formed on its surface, unlike the microstructure of the porous SBSCO cathode without applied current shown in Figure 1 (d). These particles are about 0.1 μm in size in an air atmosphere (Figure 1 (e)) and 0.15 μm in a nitrogen atmosphere (Figure 1 (f)).

The growth of fine particles on the surface of the porous cathode is due to its differing porosity. The porosity of a dense cathode was about 3% when measured at the same magnification, while the porosity of a porous cathode was about 16%. The dense cathode had a relative density of around 85% and the porous cathode had a relative density of approximately 52.5% when the relative density was measured. The dense microstructures of the dense cathode restrict the diffusion of oxygen and nitrogen gas into the bulk because of its high density. But the porous cathode with high porosity allows for easy diffusion of oxygen and nitrogen, leading to surface and internal gas diffusion [30]. Hence, the difference in gas flow diffusion around the bulk affects the generation of surface particles in the porous cathode.

In addition, Figures 1 (e) and (f) show a clear difference in microstructure when current was applied to the cathode surface in air and nitrogen atmospheres. It can be observed that when the current was applied in an air atmosphere, a higher number of fine particles are generated compared to in a nitrogen atmosphere.

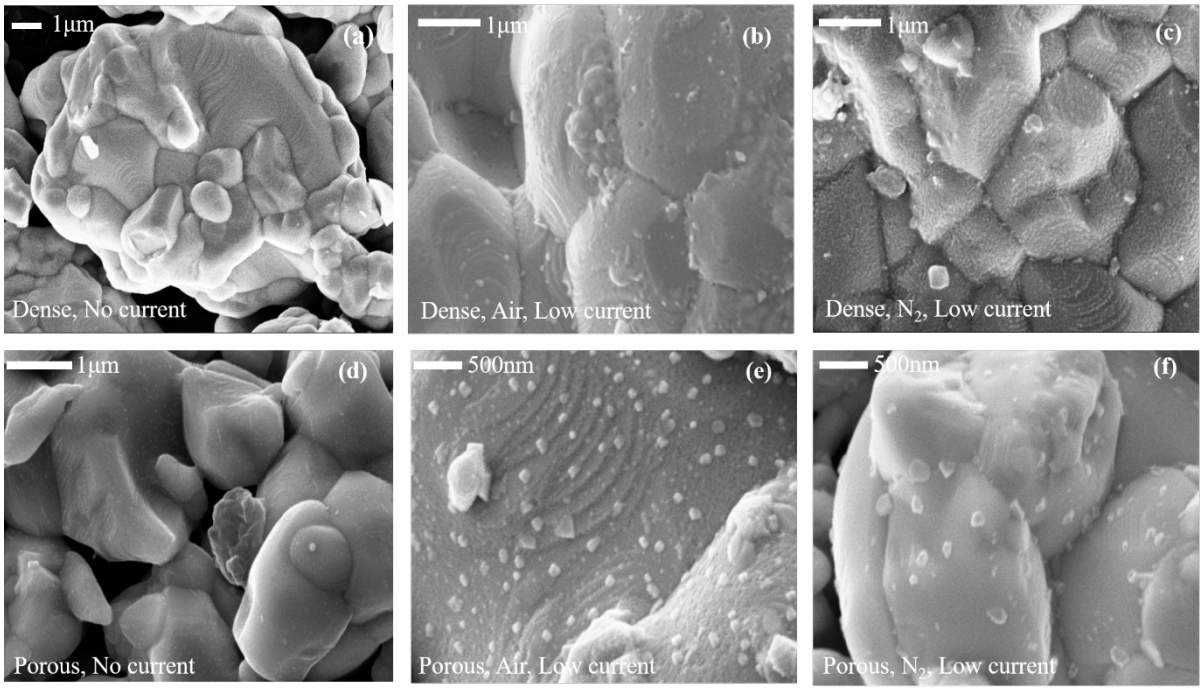

Figure 1. Microstructural differences in cathodes under air and nitrogen atmospheres with applied electrical current: Dense cathode (a) no current, (b) low current in air, and (c) low current in nitrogen atmosphere. Porous cathode (d) no current, (e) low current in air, and (f) low current in nitrogen atmosphere.

3.1.2. The effect of applied current in dense and porous cathodes

To assess the impact of the current value on the microstructure, dense and porous cathodes were analyzed with different currents applied. The corresponding applied current values can be found in Table 1.

Table1. Applied current levels for cathode microstructure and atmosphere

Microstructure of cathode	Atmosphere	Current	Amount of current
Dense type	Stagnant air	No current	-
	Air, N_2	Low current	0.1 A/min
	Air, N_2	High current	1 A/min
Porous type	Stagnant air	No current	-
	Air	Low current	0.03 A/min
		High current	0.13 A/min
	N_2	Low current	0.005 A/min
		High current	0.038 A/min

Figure 2 shows a SEM image of the cathode compared between the air and nitrogen atmospheres, focusing on the difference in the applied current value on the dense microstructure. Figure 3 presents the SEM images of the cathode according to applied current values comparing the porous microstructure between the air and nitrogen atmospheres. Compared to the microstructures of the cathode without an applied current (as seen in Figures 2 (a) and 3 (a)), distinct changes can be observed in the microstructure of the cathode with a current applied (as seen in Figures 2 (b ~ e) and 3 (b ~ e)). Specifically, when a relatively large amount of current was applied, the surface roughness of the microstructure increased, as shown in (c) and (e) of Figures 2 and 3. That is, as more current applied, more oxides generated on the surface can be observed. It can be concluded that elements inside the cathode exsolution to the surface and form oxides due to the influence of a large amount of current.

As mentioned in Part 3.1.1, when a relatively low current was applied, fine oxides appearing on the cathode surface grew more actively in an air atmosphere with a high oxygen partial pressure, which was remarkable at the porous cathode. However, as shown in (c) and (e) of Figures 2 and 3, when a high current was applied, many oxide particles were generated

regardless of the porosity and oxygen partial pressure. Therefore, the difference in the microstructure to the low and high current values can be summarized as follows. At a low current, it is affected by oxygen partial pressure and porosity. On the other hand, it can be seen that at a high current, the effect of the amount of applied current is greater than the influence of oxygen partial pressure and porosity condition.

In particular, as shown in Figure 2 (e), the exsoluted and grown particles can be seen to exist as a uniquely shaped oxide. Specifically, fine oxide exsolution particles were generated intensively in a specific part of the matrix, forming a cluster. The nanoseed particles found in this study can appear in various forms, with sizes ranging from a nanometer. In particular, Figure 2 (e) shows a nanoseed that emerged as a fine, flower-like structure with a length of approximately 400 nm, referred to as a “nanoflower”.

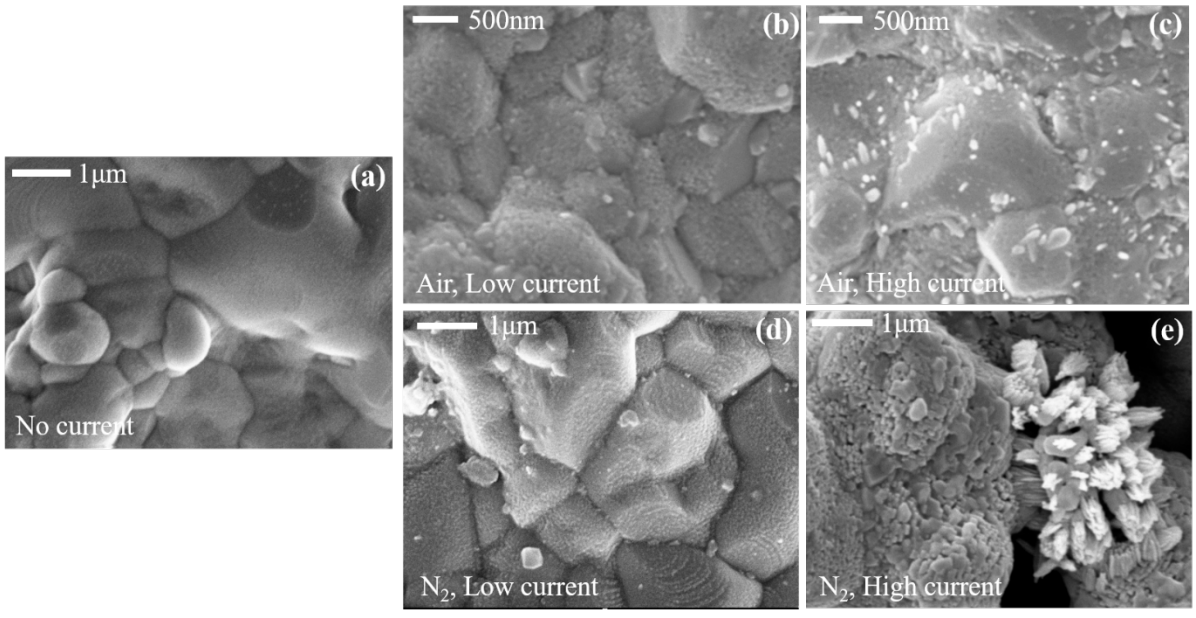

Figure 2. Characteristics of dense SBSCO microstructure cathode under different current conditions in air and nitrogen atmospheres: (a) no current (b) low current in air, (c) high current in air, (d) low current in nitrogen, and (e) high current in nitrogen.

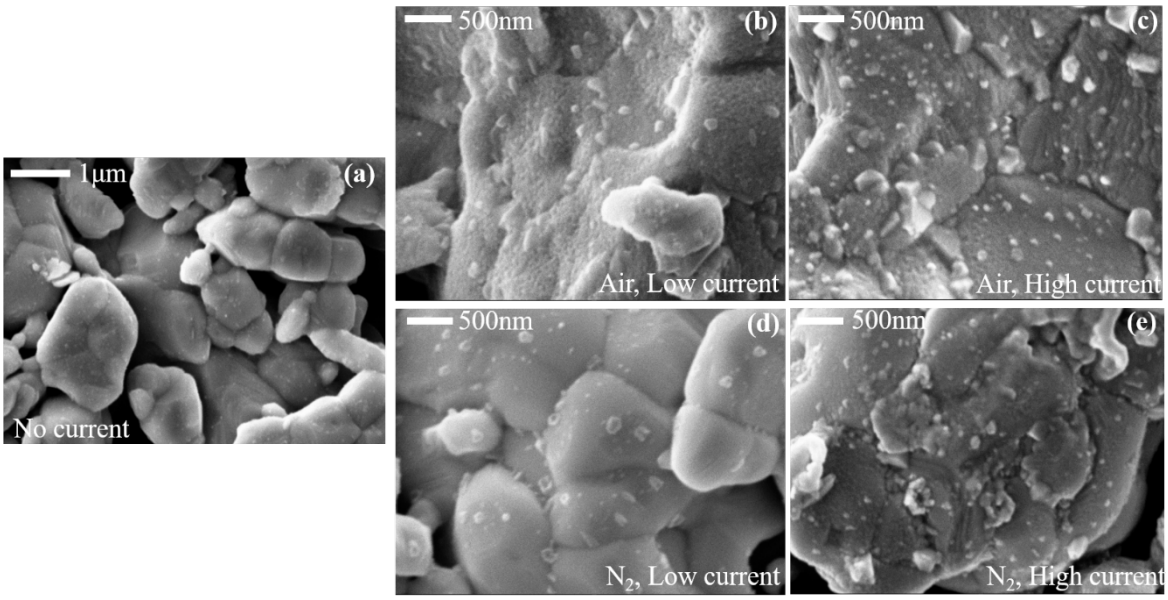

Figure 3. Characteristics of porous SBSCO microstructure cathode under different conditions in air and nitrogen atmospheres: (a) no current, in air (b) low current, (c) high current, in nitrogen (d) low current, and (e) high current.

Nanoseeds were also found in the porous cathode used in the electrical conductivity measurement conducted and are presented in Figure 4. These nanoseeds were named “nanoneedles” by our research group due to their shape, which resembles a needle among the various forms of nanoseeds in this research.

Unlike the clustered distribution of the nanoflower shown in Figure 2 (e), the nanoneedles of Figure 4 were dispersed evenly across the entire surface of the porous SBSCO matrix, and they exhibit various lengths ranging from 100 nm to 600 nm.

The microstructure of the SBSCO matrix can explain the variation in the distribution characteristics of nanoflowers and nanoneedles. The differences in their respective microstructures can be compared in Figure 2 (a) and Figure 3 (a). The dense cathode in Figure 2 (a) has a large contact area between the particles and the crystal grains due to the high degree

of connection between the particles. Therefore, the charge carriers can move easily, and the electric path can be formed continuously without obstruction. In contrast, the porous cathode in Figure 3 (a) has a small contact area between the particles and the crystal grain due to the low connect characteristic between the particles. This causes a charge bottleneck and also results in the restriction of charge carriers. In addition, the internal blocking caused by the pores between the particles hinders the formation of the electric path, resulting in a discontinuous electric path [24, 25, 31-33]. Therefore, it can be determined that the nanoflowers found in the dense microstructure are partially generated along the continuously formed electric path and are characteristic of the dense microstructure, and the nanoneedles found in the porous microstructure are generated in the entire cathode along the discontinuously constructed electric path and are characteristic of the porous microstructure.

As seen in Figure 5 and Table 2, the composition of the nanoneedles was $SmBaCo_2O_{5+d}$ (SBCO) oxide, made from Sm, Ba, Co, and O. In addition, a small amount of gold was detected due to the gold coating during SEM measurements. The SBCO exhibited an excellent electrical conductivity with a value of 570 S/cm at 200 ºC, and ASRs of approximately 0.1 Ωcm^2 at 700 ºC. When used in a 5:5 weight ratio with $Ce_{0.9}Gd_{0.1}O_{2-d}$ (CGO91), the ASR reduced to 0.05 Ωcm^2 at 700°C [36]. After observation of the formation of SBCO nanoneedles with these unique characteristics, the electrical conductivity results of the cathode with and without nanoneedles are summarized in section 3.2.

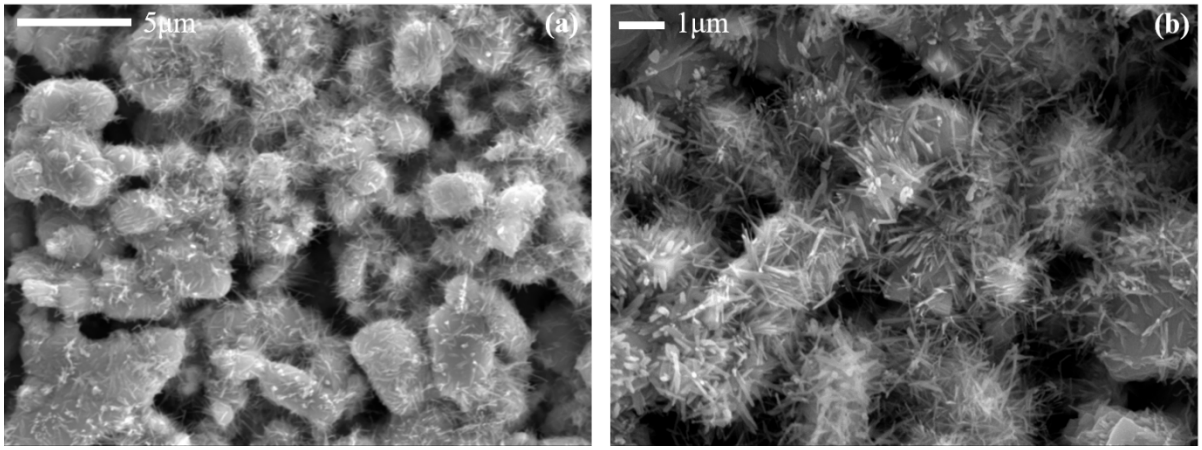

Figure 4. Nanoneedles in porous microstructure cathode

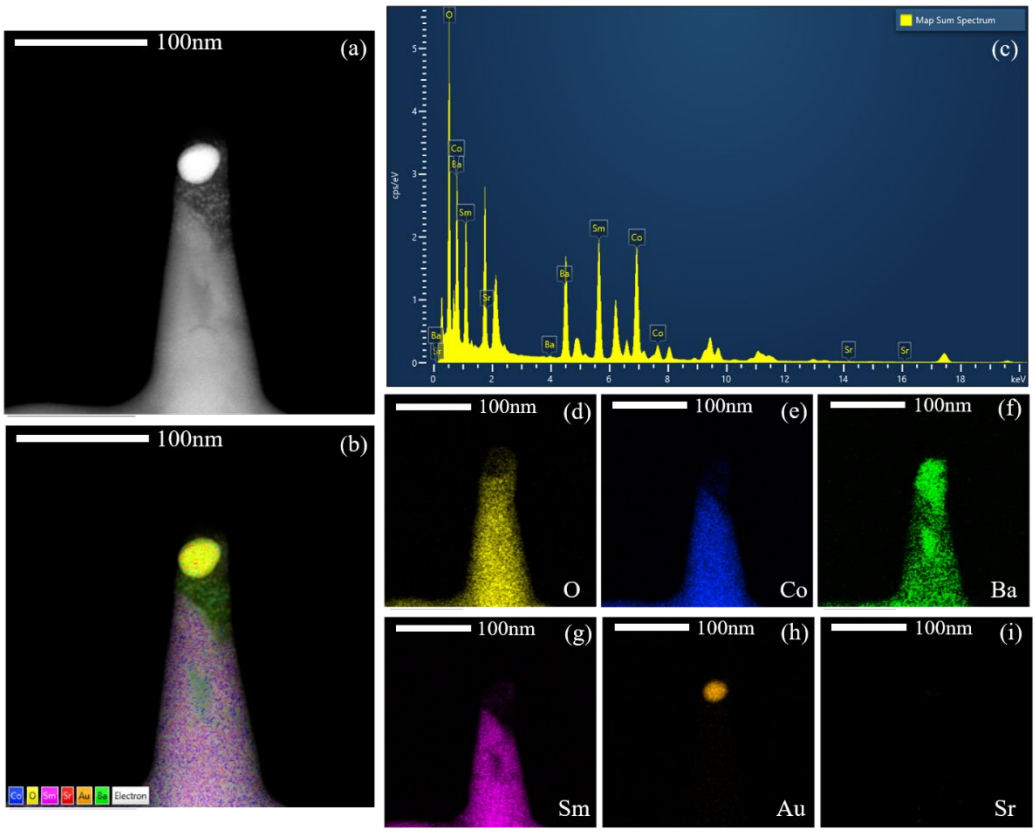

Figure 5. EDS analysis of nanoneedles: (a) Nanoneedle TEM image, and (b ~ i) result of EDS

Table 2. Atomic percentage of nanoneedles analyzed by EDS

Element	Atom%
O	61.89
Co	14.66
Ba	7.56
Sm	15.88
Total	100.00

As such, nanoseeds exhibit a range of shapes and sizes. The different types of nanoseeds are summarized in Figure 6, including nanosheets [34] and nanocubes [35] found in previous literature, as well as the nanoflowers and nanoneedles found in this study.

The nanoflowers (Figure 2 (e)) in this study were formed under a nitrogen atmosphere and high current in the dense cathode. Meanwhile, a high current in the porous cathode generated nanoneedles (Figure 4) under both air and nitrogen conditions. As such, both the nanoflowers and nanoneedles were forms of nanoseeds, but their shape characteristics and formation conditions were distinct from each other.

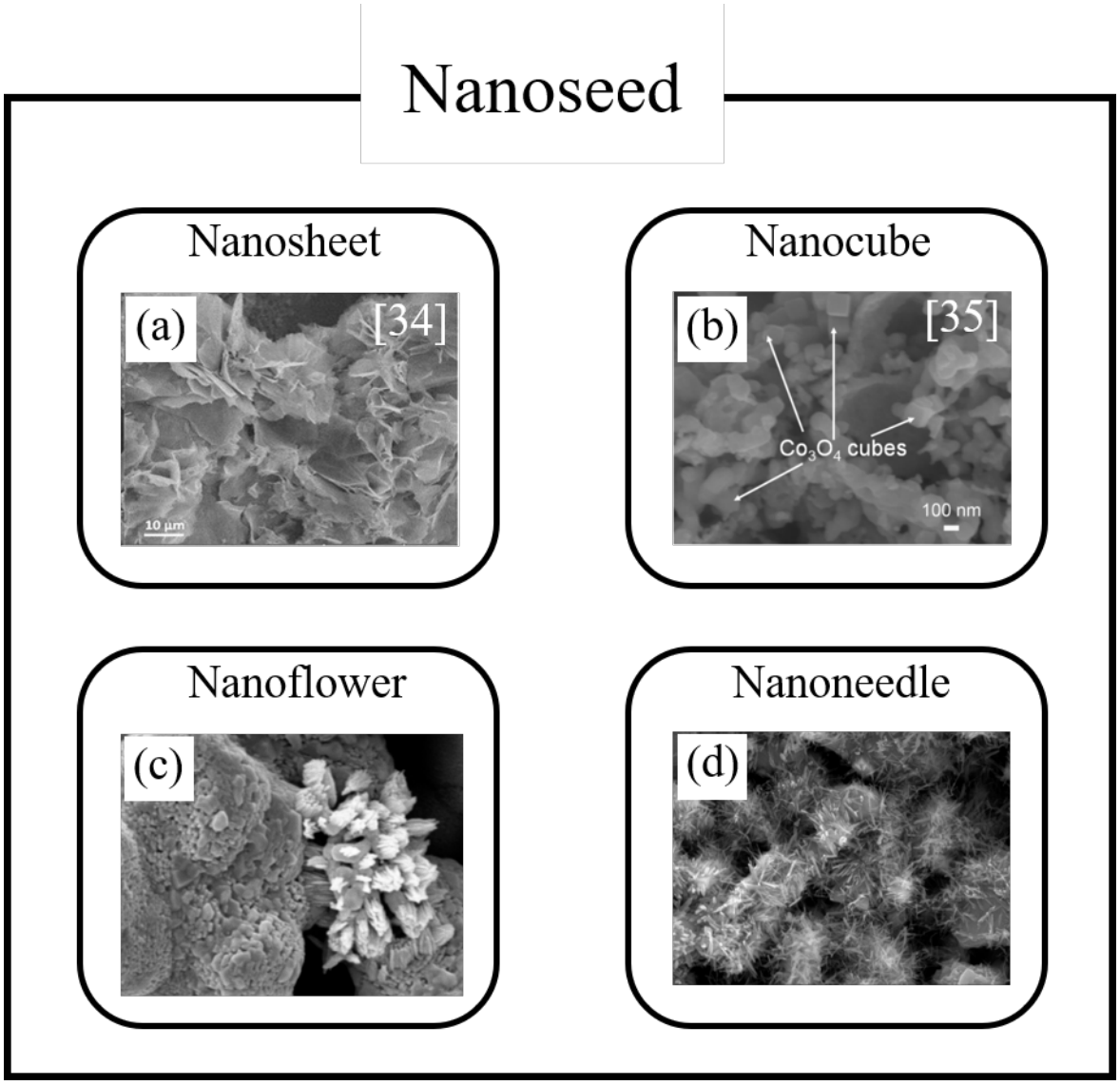

Figure 6. Types of nanoseed: (a) nanosheet [34] and (b) nanocube [35]. (c) nanoflower, and (d) nanoneedle found in this study.

3.2. Electrical conductivities with respect to the applied current

Comparing the microstructural characteristics with respect to the applied current, nanoseeds were not generated when a low current value was applied. On the other hand, the generation of nanoseeds was confirmed when a high current value was applied, and the electrical

conductivity was measured to verify the effect of this microstructural difference on the cathode.

As shown in Figure 4, it was determined that the nanoneedles generated on most of the cathode surface would directly affect the cathode performance. Therefore, porous cathodes with nanoneedles (nanoneedle cathode) and porous cathodes without nanoneedles (normal cathode) were used for the electrical conductivity measurement. This experiment confirmed that no nanoneedles were produced when a low current was applied, but they were found on the cathode used in the electrical conductivity experiment when a high current was applied. Therefore, in the case of the porous cathode, it was determined that a difference in electrical conductivity due to the presence of nanoneedles could be confirmed through the experimental results showing the same conductivity regardless of the amount of applied current [24], and electrical conductivity measurement and analysis were conducted.

Regarding the overall electrical characteristics, electrical conductivity exhibits typical semiconductor behavior, with increased conductivity as the temperature rises, regardless of the presence of nanoneedles. The electrical conductivity values measured during the cooling process (Down) were higher than those measured during the heating process (Up). For example, in the case of the nanoneedle cathode under an air atmosphere at 700 ºC, the conductivity value measured during the cooling process (■) was approximately 238 S/cm. In contrast, the value measured during the heating process (■) was about 222 S/cm. The difference in the electrical conductivity value is due to the measurement being conducted after sufficient thermal activation at a high temperature of 900 ºC to allow for the movement of charge carriers in the cathode [37].

The difference in electrical conductivity due to the change in oxygen partial pressure indicates that it is a typical P-type conductor, as it shows higher electrical conductivity in an air atmosphere compared to a nitrogen atmosphere. For example, in the case of the nanoneedle

cathode that underwent a heating process, the electrical conductivity measured in an air atmosphere (■) was approximately 222 S/cm at 700 ºC. In contrast, the conductivity measured in a nitrogen atmosphere (■) was about 175 S/cm at 700 ºC. Therefore, the nanoneedle cathode has higher electrical conductivity in the air atmosphere.

Additionally, the electrical conductivity varies based on the presence of nanoneedles. At 700 °C, under a cooling process and air atmosphere, the electrical conductivity of the nanoneedle cathode (■) was approximately 238 S/cm, while the conductivity of the normal cathode (□) was about 136 S/cm.

Accordingly, Figure 7 shows that the nanoneedle cathode exhibits higher electrical conductivity values than the normal cathode in all the measured conditions.

The Arrhenius equation [$\sigma = A/kT \exp(-E_a / kT)$] was employed to calculate the activation energy using the measured electrical conductivity. From the results of electrical conductivity measurement, the slope in the ranges of 350 ºC to 650 ºC, which is linear in all conditions, was used and the activation energy values with respect to the presence of nanoneedles are summarized in Figure 7, and Table 4. The activation energy values of the nanoneedle cathode ranged from 0.111 eV ~ 0.126 eV across all experiments. On the other hand, the activation energy values for the normal cathode varied from about 0.133 eV to 0.177 eV in all conditions. This indicates that the nanoneedle cathode exhibits an enhanced electrochemical reaction on its surface compared to the normal cathode. This implies that the mobility of holes, which act as the primary charge carrier, is more efficient in the nanoneedle cathode than in the normal cathode. The formation of nanoneedles increases the total surface area of the cathode, providing more pathways for hole mobility, resulting in an overall increase in hole movement [38, 39].

Therefore, it was confirmed that the presence of nanoneedles directly affects the performance of the cathode, leading to a significant improvement in electrical conductivity due

to the increase in hole mobility.

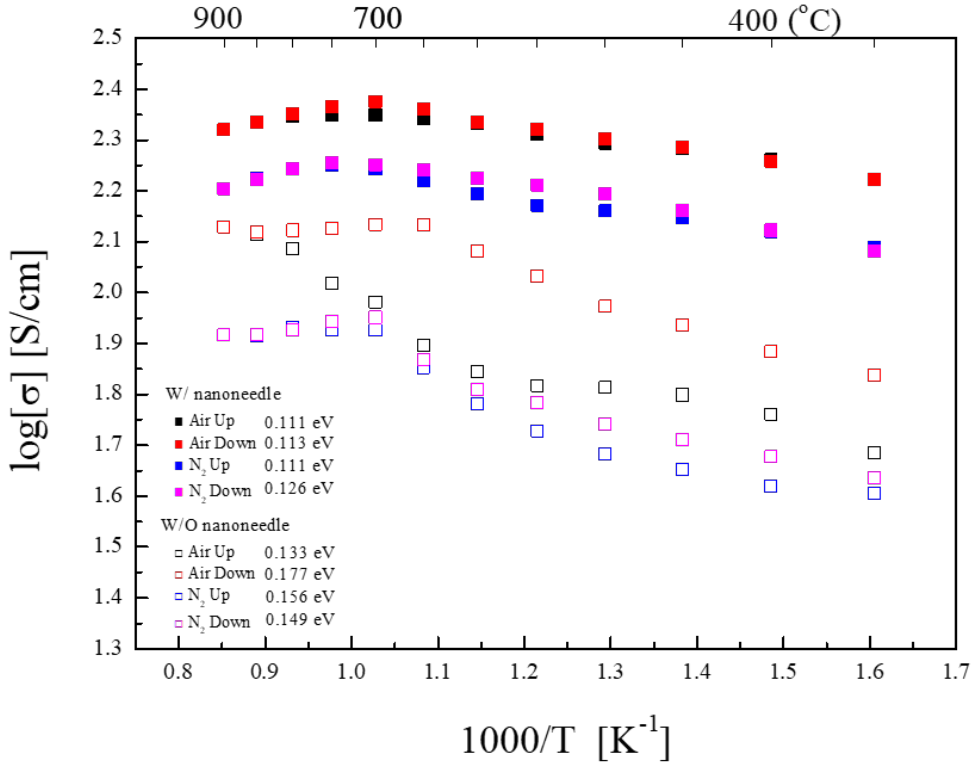

Figure 7. Electrical conductivities with respect to the presence of nanoneedles.

Table 3. Electrical conductivity variation with respect to the presence of nanoneedles

Sample	Atmosphere	Electrical conductivity (S/cm)				
		600ºC	650ºC	700ºC	750ºC	800ºC
W/ Nanoneedle	Air Up	212.75	218.54	221.55	221.55	220.22
	Air Down	217.22	230.28	237.52	232.21	224.25
	N_2 Up	156.30	165.80	174.96	178.15	175.20
	N_2 Down	168.18	174.14	178.34	180.02	175.29
W/O Nanoneedle	Air Up	69.83	78.74	95.67	104.35	122.13
	Air Down	120.54	136.18	136.18	133.78	132.64
	N_2 Up	60.48	71.30	84.30	84.49	85.27
	N_2 Down	64.38	74.01	89.42	87.77	84.30

Table 4. Activation energies with respect to the presence of nanoneedles (350 ºC ~ 650 ºC)

Sample	Atmosphere	Activation Energy(eV)
W/ Nanoneedle	Air Up	0.111
	Air Down	0.113
	N_2 Up	0.111
	N_2 Down	0.126
W/O Nanoneedle	Air Up	0.133
	Air Down	0.177
	N_2 Up	0.156
	N_2 Down	0.149

4.Conclusion

The main goal of this research was to investigate the relationship between microstructural changes and electrical conductivity in a layered perovskite SBSCO cathode when different levels of current (no current, low current, high current) were applied.

When applying a low current to the two types of cathodes (dense and porous SBSCO cathode), it was found that finer particles formed on the surface of the porous cathode compared to the dense cathode. Additionally, more fine particles were formed in an air atmosphere compared to a nitrogen atmosphere.

Differences in microstructure were also observed under different current values. It was confirmed that the number of particles increased and grew in the order of no current, low current, and high current. In this case, nanoseeds were discovered when a high current was applied to the dense and porous cathode. The appearance of nanoneedles, a type of nanoseed, was observed across the entire surface of the cathode. It was found that the nanoneedles were composed of the chemical compound $SmBaCo_2O_{5+d}$ (SBCO).

The electrical conductivities of the nanoneedle cathode and the normal cathode were 238 S/cm

and 136 S/cm at 700 ºC, in the case of the porous cathodes. This clearly indicates that the nanoneedles contribute to improved electrical conductivity. Furthermore, when the activation energies were calculated through the measured electrical conductivity value, the activation energy value of the nanoneedle cathode was 0.111 eV (Air Down) and that for the normal cathode was 0.133 eV. These results also suggest that nanoneedles aid the movement of holes, which are the primary charge carriers of the cathode.

Acknowledgments

This work was supported by the National Research Foundation of Korea grant funded by the Ministry of Science and ICT of the Korean government (No. 2019R1A2C1087534 and No.2022M3H4A1A04080547).

Declaration of competing interest

The authors declare that they have no known competing financial interests or personal relationships that could have appeared to influence the work reported in this paper.

References

[1]Abdalla AM, Hossain S, Azad AT, Petra PMI, Begum F, Eriksson SG, et al. Nanomaterials for solid oxide fuel cells: A review. Renew Sustain Energy Rev 2018;82:353–68.

[2]Davis SJ, Lewis NS, Shaner M, Aggarwal S, Arent D, Azevedo IL, et al. Net-zero emissions energy systems. Science 2018;360.

[3]Priya SD, Selvakumar AI, Nesaraj AS. Overview on ceramic and nanostructured materials for solid oxide fuel cells (Sofcs) working at different temperatures. J Electrochem Sci Technol 2020;11:99–116.

[4]Szmyd JS. World Energy Resources and New Technologies. Pap Glob Chang IGBP 2016;23:21–35.

[5]Nikonov A V., Kuterbekov KA, Bekmyrza KZ, Pavzderin NB. A brief review of conductivity and thermal expansion of perovskite-related oxides for SOFC cathode. Eurasian J Phys Funct Mater 2018;2:274–92.

[6]Du Y, Finnerty C, Jiang J. Thermal Stability of Portable Microtubular SOFCs and Stacks. J Electrochem Soc 2008;155:B972.

[7]Fallah Vostakola M, Amini Horri B. Progress in Material Development for Low-Temperature Solid Oxide Fuel Cells: A Review. Energies 2021;14:1280.

[8]Zhou Y, Lü Z, Li J, Xu S, Xu D, Wei B. The electronic properties and structural stability of $LaFeO_3$ oxide by niobium doping: A density functional theory study. Int J Hydrogen Energy 2021;46:9193–8.

[9]Zhou X, Zhou F. Application of $La_{0.3}Sr_{0.7}Fe_{0.7}Ti_{0.3}O_{3-\delta}$/GDC electrolyte in LT-SOFC. Int J Hydrogen Energy 2021;46:9988–95.

[10]Zhang X, Espinoza M, Li T, Andersson M. Parametric study for electrode microstructure

influence on SOFC performance. Int J Hydrogen Energy 2021;46:37440–59.

[11]Xu J, Wan S, Wang Y, Huang S, Yuan Z, Chen F, et al. Enhancing performance of molybdenum doped strontium ferrite electrode by surface modification through Ni infiltration. Int J Hydrogen Energy 2021;46:10876–91.

[12]Lu Y, Mushtaq N, Yousaf Shah MAK, Irshad MS, Rauf S, Yousaf M, et al. $Ba_{0.5}Sr_{0.5}Fe_{0.8}Sb_{0.2}O_{3-\delta}$-$Sm_{0.2}Ce_{0.8}O_{2-\delta}$ bulk heterostructure composite: A cobalt free Oxygen Reduction Electrocatalyst for low-temperature SOFCs. Int J Hydrogen Energy 2022;47:38348–60.

[13]Jiang SP. Development of lanthanum strontium cobalt ferrite perovskite electrodes of solid oxide fuel cells – A review. Int J Hydrogen Energy 2019;44:7448–93.

[14]Weber A, Ivers-Tiffée E. Materials and concepts for solid oxide fuel cells (SOFCs) in stationary and mobile applications. J Power Sources 2004;127:273–83.

[15]Skinner SJ. Recent advances in perovskite-type materials for solid oxide fuel cell cathodes. Int J Inorg Mater 2001;3:113–21.

[16]Yang Z, Guo M, Wang N, Ma C, Wang J, Han M. A short review of cathode poisoning and corrosion in solid oxide fuel cell. Int J Hydrogen Energy 2017;42:24948–59.

[17]Yoo S, Choi S, Kim J, Shin J, Kim G. Investigation of layered perovskite type $NdBa_{1-x}Sr_xCo_2O_{5+\delta}$ (x = 0, 0.25, 0.5, 0.75, and 1.0) cathodes for intermediate-temperature solid oxide fuel cells. Electrochim Acta 2013;100:44–50.

[18]Chen D, Ran R, Zhang K, Wang J, Shao Z. Intermediate-temperature electrochemical performance of a polycrystalline $PrBaCo_2O_{5+\delta}$ cathode on samarium-doped ceria electrolyte. J Power Sources 2009;188:96–105.

[19]Kim G, Wang S, Jacobson AJ, Reimus L, Brodersen P, Mims CA. Rapid oxygen ion diffusion and surface exchange kinetics in $PrBaCo_2O_{5+x}$ with a perovskite related structure and

ordered a cations. J Mater Chem 2007;17:2500–5.

[20]Woo SH, Song KE, Baek SW, Kang H, Choi W, Shin TH, et al. Pr- and Sm-substituted Layered Perovskite Oxide Systems for IT-SOFC Cathodes. Energies 2021;14:6739.

[21]Song SW, Choi WS, Kang H, Baek SW, Azad AK, Park JY, et al. Synthesis and electrochemical properties of layered perovskite substituted with heterogeneous lanthanides for intermediate temperature-operating solid oxide fuel cell. Int J Hydrogen Energy 2018;43:11378–85.

[22]Ding D, Liu M, Liu M. Enhancing SOFC Electrode Performance Through Surface Modification. ECS Trans 2013;57:1801–10.

[23]Kim JH, Cassidy M, Irvine JTS, Bae J. Electrochemical investigation of composite cathodes with $SmBa_{0.5}Sr_{0.5}Co_2O_{5-\delta}$ cathodes for intermediate temperature-operating solid oxide fuel cell. Chem Mater 2010;22:883–92.

[24]Song KE, Schlegl H, Kim CG, Baek KS, Lim YR, Nam JH, et al. Electrical conductivity properties of porous $SmBaCo_2O_{5+d}$ and $SmBa_{0.5}Sr_{0.5}Co_2O_{5+d}$ layered perovskite oxide systems for solid oxide fuel cell. Ceram Int 2022;48:28649–58.

[25]Song KE, Schlegl H, Kang H, Choi W, Kim JH. Electrochemical characteristic of non-stoichiometric $SmBa_{0.45}Sr_{0.5}Co_2O_{5+d}$ layered perovskite oxide system for IT-SOFC cathode. Int J Hydrogen Energy 2023;48:17664–76.

[26]Baek KS, Baek SW, Kang H, Choi W, Park JY, Saxin S, et al. Electrical conductivity characteristics of Sr substituted layered perovskite cathode ($SmBa_{0.5}Sr_{0.5}Co_2O_{5+d}$) for intermediate temperature-operating solid oxide fuel cell. Ceram Int 2022;48:15770–9.

[27]Song KE, Lee JW, Lim YR, Baek SW, Shin TH, Lee S, et al. Influence of microstructure and applied current on the electrical conductivity of $SmBaCo_2O_{5+d}$ cathode in solid oxide fuel cell. Int J Hydrogen Energy 2022;47:15875–86.

[28]Kim CG, Woo SH, Song KE, Baek SW, Kang H, Choi WS, et al. Enhanced Electrochemical Properties of Non-stoichiometric Layered Perovskites, $Sm_{1-x}BaCo_2O_{5+d}$, for IT-SOFC Cathodes. Front Chem 2021;9:633868.

[29]Kim JH, Cassidy M, Irvine JTS, Bae J. Advanced Electrochemical Properties of $LnBa_{0.5}Sr_{0.5}Co_2O_{5+\delta}$ (Ln=Pr, Sm, and Gd) as Cathode Materials for IT-SOFC. J Electrochem Soc 2009;156:B682.

[30]Riazat M, Baniassadi M, Mazrouie M, Tafazoli M, Moghimi Zand M. The Effect of cathode Porosity on Solid Oxide Fuel Cell Performance. Energy Equip Syst 2015;3:25–32.

[31]Park KY, Lim JM, Luu NS, Downing JR, Wallace SG, Chaney LE, et al. Concurrently Approaching Volumetric and Specific Capacity Limits of Lithium Battery Cathodes via Conformal Pickering Emulsion Graphene Coatings. Adv Energy Mater 2020;10:1–11.

[32]Paydar S, Shariat MH, Javadpour S. Investigation on electrical conductivity of LSM/YSZ8, LSM/$Ce_{0.84}Y_{0.16}O_{0.96}$ and LSM/$Ce_{0.42}Zr_{0.42}Y_{0.16}O_{0.96}$ composite cathodes of SOFCs. Int J Hydrogen Energy 2016;41:23145–55.

[33]El Khal H, Cordier A, Batis N, Siebert E, Georges S, Steil MC. Effect of porosity on the electrical conductivity of LAMOX materials. Solid State Ionics 2017;304:75–84.

[34]Badreldin A, Abusrafa AE, Abdel-Wahab A. Oxygen-Deficient Cobalt-Based Oxides for Electrocatalytic Water Splitting. ChemSusChem 2021;14:10–32.

[35]Xu X, Wang C, Fronzi M, Liu X, Bi L, Zhao XS. Modification of a first-generation solid oxide fuel cell cathode with Co_3O_4 nanocubes having selectively exposed crystal planes. Mater Renew Sustain Energy 2019;8:1–8.

[36] Kim, J. H., Bae, J., Cassidy, M., Connor, P. A., Zhou, W., & Irvine, J. $SmBaCo_2O_{5+d}$ and $LnBa_{0.5}Sr_{0.5}Co_2O_{5+\delta}$, Potential Cathode Materials for IT-SOFC. Ecs Transactions 2009;25:2707-15.

[37]PARK JS, KIM HG. Electrical Conductivity and Defect Models of MgO-Doped Cr_2O_3. J Am Ceram Soc 1988;71:173–6.

[38]Suchaneck G, Artiukh E. Nonstoichiometric Strontium Ferromolybdate as an Electrode Material for Solid Oxide Fuel Cells. Inorganics 2022;10.

[39]Merkulov O V., Markov AA, Naumovich EN, Shalaeva E V., Leonidov IA, Patrakeev M V. Non-uniform electron conduction in weakly ordered $SrFe_{1-x}Mo_xO_{3-\delta}$. Dalt Trans 2019;48:4530–7.